Desalination and Water Treatment
www.deswater.com

doi: 10.5004/dwt.2023.29872

309 (2023) 8–21
October

RO-TRACK: data driven predictive analytics for seawater reverse osmosis desalination plants

Muhammad Ghifari Ridwan, Thomas Altmann, Ahmed Yousry, Hussain Basamh, Ratul Das*

Innovation and New Technology, ACWA Power, 41st Floor, The One Tower, Sheikh Zayed Road, Dubai, UAE, email: rdas@acwapower.com (R. Das)

Received 16 August 2023; Accepted 29 August 2023

ABSTRACT

One of the major sources of operational cost in seawater reverse osmosis is towards membrane replacement. While membrane replacement is certainly unavoidable due to irreversible fouling, its rate can be minimized thorough operational changes. One common action to mitigate fouling is cleaning in place (CIP) – circulating chemicals on the membrane to dissolve the fouling matter. However, CIP efficacy is highly dependent on the timing and types of the foulant. Further, the current procedure to investigate the type of foulant can take months as the membrane autopsy procedure requires sophisticated analysis. Here, we present data-driven analytics that can generate insights about the potential type of foulant and provides a timeline for the next CIP based on the membrane performance parameters. This approach is based on our insight's generator framework developed using historical data, coupled with machine learning algorithms and operational knowledge tree.

Keywords: Reverse osmosis; Monitoring; Diagnostic; Cleaning in place; Data-driven analytics; Forecasting

1. Introduction

Freshwater nourishes and sustains life, incessant population growth demands for a greater supply of freshwater [1,2]. While the advent and continuous improvement of freshwater generation technologies have existed, the rate is slowing down [1]. The transition from utilizing low-grade energy (heat) to high-grade energy (pressure) for desalination drove down the specific energy consumption (SEC) significantly from ~20 to ~3 kWh/m^3 during the last 20 y, however, no significant improvement has been made over the last 5 y [3]. Seawater reverse osmosis (SWRO) is considered the most efficient method for generating freshwater from seawater [4,5]. The process separates inorganic salts from pressurized seawater through a semi-permeable membrane [6–10], the potential energy from seawater overcomes the osmotic barrier. It is apparent that current systems and technologies is already approaching the theoretical limit of the process, which is around ~1.5 kWh/m^3 [11]. To further drive-down SEC, several processes have been attempted, including membrane performance improvement [12–15], and novel system design [16–18]. A paradigm shift is needed for further improvement of efficiency.

One such avenues for higher energy efficiency is employing digitalization to enable better design, operation, and maintenance [19,20]. The utilization of the internet of things (IoT), automation, and predictive analytics in many industrial sectors including desalination have shown tremendous evidence to maximize process and plant efficiency, thereby reducing operational costs [20–25]. To embark on the digitalization journey, efforts are also supported by increasingly accurate and robust sensors, which enable real-time accurate data acquisition. This advancement unlocks the door to exploit real-time data with automated data processing

* Corresponding author.

Presented at the European Desalination Society Conference on Desalination for the Environment: Clean Water and Energy, Limassol, Cyprus, 22–26 May 2023

and advanced analytics including statistics and machine learning for optimization, diagnosis, and prediction. One of the direct utilizations of this infrastructure in the desalination industry is in the membrane performance monitoring system. Membrane replacement due to the fouling or other irreversible damage is one of the highest capital and operational cost component for SWRO systems, their real time performance monitoring system requires further optimization [26–30]. In response, we developed an automated membrane performance tracking and diagnostics system. This system is established with data pipelines from more than 20 seawater desalination plants, with a total production capacity above 5 million·m^3/d. The system is capable of providing valuable insights to the operators by supplying important information such as forecasting the timeline for the next cleaning in place (CIP), and detection of root cause for membrane performance decline. These insights enable preventive and corrective actions to optimize the SWRO plant's day-to-day operations and further reduceoperational cost [31].

2. Methods

RO-TRACK works based on three main steps: (i) data ingestion and processing, (ii) information extraction, and (iii) insights generation (Fig. 1). The data ingestion consists of data acquisition, data upload, data cleaning, validation, gap filling, and data storage. Subsequently, the data is supplied to the normalization module for data normalization. From the normalized data, advanced pattern recognition and the diagnostic algorithm are employed to generate insights into the plant's performance.

2.1. Data ingestion and processing

The data ingestion starts by acquiring data from the desalination plant, through distributed control system. Acquired data is then uploaded to the cloud storage. While the raw data is directly stored, the raw data is subsequently processed by removing non-numeric values and outliers. The outlier is detected based on ± standard deviation (σ) of past 6 months data and the data file that is being uploaded. The processed data is stored as clean data. Subsequently, the missing parameters necessary for data normalization are calculated using mass and energy balance equation, this process is called gap analysis. The gap analysis is tailored based on the plant configuration and sensors availability. We provided the gap analysis on Supplementary Information Section 9.

2.2. Data normalization

The validated and clean data is used for data normalization. Data normalization enables a fair and reliable comparison of initial membrane performance with its current and historical performance [32–34]. The typical output of data normalization is (i) normalized salt passage (NSP), (ii) normalized differential pressure (NDP), and (iii) normalized permeate flow (NPF). In addition to this, it also provides additional parameters including (i) water transport coefficient, (ii) salt transport coefficient, and (iii) specific flux to provide additional insights on real-time membrane performance. We are providing the normalization method used for TORAY membranes and the standard method used by American Society for Testing and Materials (ASTM D 4516) [35,36].

Data normalization by TORAY is done mainly for permeate flow, salt passage, and differential pressure. It is performed by referring to the initial system performance (t = 0). As described in Table 1, NPF and NDP are common parameters in all approaches. However, intermediate calculations for osmotic pressures and temperature correction factors shall be considered for each approach. In addition, we provide detail calculations for membrane performance normalization from SI section 1–8.

2.3. Specific membrane energy consumption

Typically, large scale reverse osmosis (RO) desalination consists of more than 10 racks. In daily operations, the operators require to oversee those racks. Here, we are using simple yet effective parameter to quickly comparing the membrane performance. We use specific membrane energy consumption. With specific membrane energy consumption, the operator can get an indication to focus on specific train. Membrane energy consumption, $E_{membrane}$, is a parameter that calculate the quantity of energy being

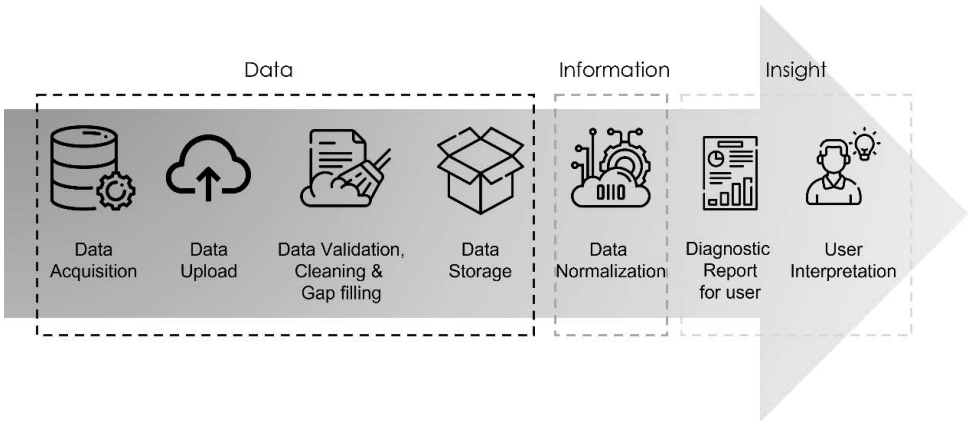

Fig. 1. General description of monitoring and diagnostic process.

Table 1
Normalized parameter formulas from TORAY and ASTM methods

TORAY method	ASTM method
$\mathrm{NDP} = \mathrm{DP} \times \left(\frac{Q_{\mathrm{FBA},r}}{Q_{\mathrm{FBA},t}}\right)^{\mathrm{DP3}} \times \left(\frac{\mu_r}{\mu_t}\right)^{\mathrm{DP6}}$	Not available
$\mathrm{NPF} = Q_{P,t} \times \frac{\mathrm{NetDP}_r \times \mathrm{TCF}_r}{\mathrm{NetDP}_t \times \mathrm{TCF}_t}$	
$\mathrm{NSP} = \mathrm{SP}_t \times \frac{Q_{P,t} \times \mathrm{TCF}_{\mathrm{Salt},0} \times \mathrm{CF}_{\mathrm{lm},0} \times C_{F,t}}{Q_{P,0} \times \mathrm{TCF}_{\mathrm{Salt},t} \times \mathrm{CF}_{\mathrm{lm},t} \times C_{F,0}}$	$\mathrm{NSP} = \frac{\mathrm{EPF}_t}{\mathrm{EPF}_r} \times \frac{\mathrm{STCF}_r}{\mathrm{STCF}_t} \times \frac{C_{\mathrm{FC},r}}{C_{\mathrm{FC},t}} \times \frac{C_{F,t}}{C_{F,r}} \times \mathrm{SP}_t$

consumed by the membrane to separate water from salt. E_{membrane} is calculated by taking the difference of feed energy, E_{feed}, and permeate, E_{permeate} and brine energy, E_{brine}. Each energy component is the product of the flowrate and pressure, $E_{\mathrm{component}} = Q_{\mathrm{component}} \times P_{\mathrm{component}}$. Further, the membrane energy specific consumption is specified by dividing it with permeate flowrate, Q_{permeate}.

2.4. Membrane CIP prediction and diagnostics

The normalized data and supplementary diagnostic indicators are combined to provide insights on membrane performance. To conduct the CIP prediction, the real-time data is smoothened to ensure better trend recognition and forecasting processes. Upon the completion of this process, the data is fed to the forecasting and trend recognition algorithm to give the CIP prediction and diagnostic output. The diagnostic output is generated from the understanding of the trend of specific parameters. The domain knowledge from the membrane autopsy and operational data from plants enables sufficient confidence in diagnostic recommendations. The process of the data analytics is provided in Fig. 2.

For the trend recognition process, we utilize the Mann–Kendall (MK) trend test [37,38]. The test is sequentially comparing the magnitude of the next and previous values, $S = \sum_{k=1}^{n-1} \sum_{j=k+1}^{n} f\left(x_j - x_k\right)$. Upon the comparison, a dedicated value is assigned depending on the comparison result: (i) $f(x_j - x_k) = 1$ if $x_j - x_k > 0$, (ii) $f(x_j - x_k) = 0$ if $x_j - x_k = 0$, and (iii) $f(x_j - x_k) = -1$ if $x_j - x_k < 0$ [37,38]. A positive value of S indicates an increasing trend, while a negative value of S indicates a decreasing trend. If the value of S is equal to zero, the trend is neither increasing nor decreasing. The advantage of this test is the dataset does not require to conform to conform any distribution form. The recognized trend from specific data will then be fed into the diagnostic tree system. The diagnostic tree system enables the transformation of multiple trends into a possible root cause of membrane performance decline. The diagnostic tree is developed based on ACWA power's extensive experience in the desalination sector (Fig. 3).

In addition to the diagnostic system, RO-TRACK also provides the user with the CIP timeline prediction based on the NPF and NDP value. We are using multiple regression options on ForecastAutoreg to estimate the CIP timing based on the maximum allowable value of NPF and NDP.

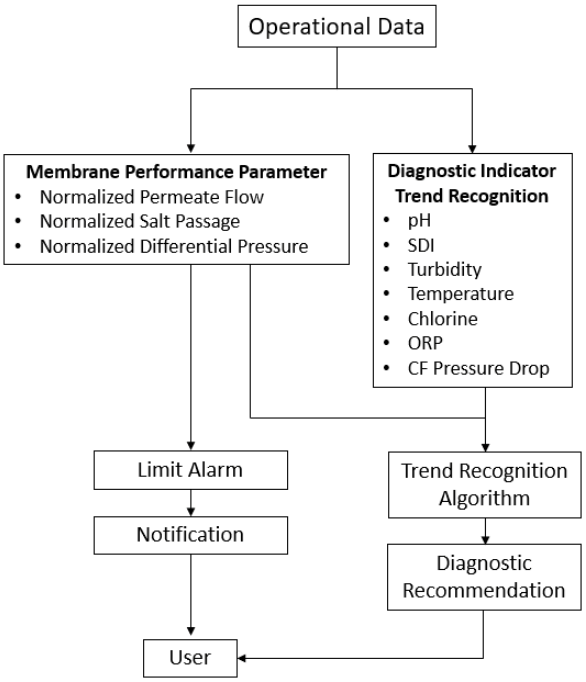

Fig. 2. Specific description of monitoring and diagnostic process.

In this paper, we are presenting the regression using the ridge regressor.

3. Result and discussion

3.1. RO desalination plant description

As a test case, we are using the operational data from one of RO trains from one of the ACWA power RO desalination plant assets. The desalination plant produces > 200,000 m^3/d located in the shore of the Gulf of Arabia. The detailed process flow diagram in Fig. 4. In the pretreatment, the plant utilizes dissolved air flotation (DAF) and dual media pressurized filter (DMPF). Along this pretreatment operation, series of chemicals are dosed including $FeCl_3$, $NaHSO_3$, and antiscalant. In between 1st pass and 2nd pass of RO section, NaOH and antiscalant are dosed for better boron removal and prevent scaling at high pH, respectively. Upon the RO

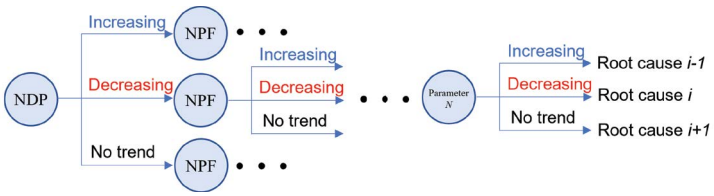

Fig. 3. Diagnostic tree based on the trend recognition of specific parameters.

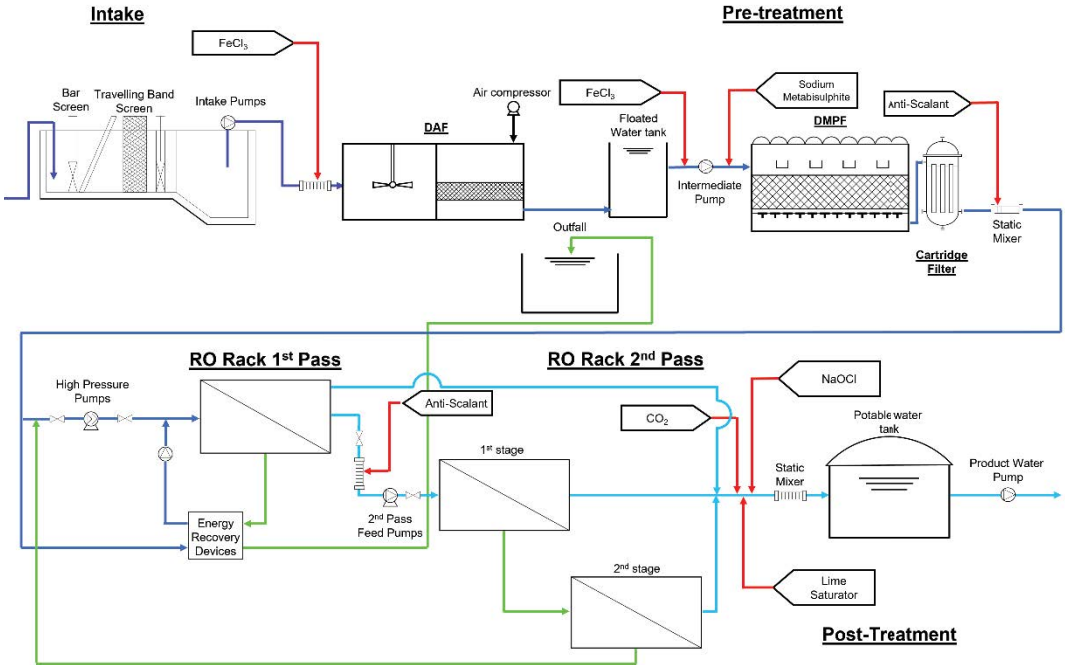

Fig. 4. Process flow diagram of desalination plant used for RO-TRACK.

separation process, permeate water is being treated with CO_2, lime, and NaOCl. These chemicals are intended to meet specific requirement of potable water including the hardness and free chlorine limit.

3.2. Reverse osmosis operational data

Several operational parameters from a SWRO plant are shown in Fig. 5. The data is obtained from the mid of March to the end of May 2021. The inlet seawater temperature fluctuates on a daily basis, in which during this specific period of data collection, the inlet temperature is gradually increasing from 21°C to 34°C. In addition, the inlet seawater conductivity is gradually decreasing from 59 to 56 mS/cm while the permeate conductivity is increasing from 750 to 1,300 μS/cm. It is important to notice that there are significant changes in permeate conductivity at the end of April 2021. This change is due to the increase in inlet temperature of the seawater feed, which reduces the viscosity of the water and allows for a greater salt passage through the membranes.

3.3. Reverse osmosis data normalization

In this section, we discuss the result of data normalization in graphical form (Fig. 6). We normalized the data using TORAY correlation as per the membrane type utilized in operations. The results display the data from mid of March 2021 to the end of May 2021. In between the result, the CIP is conducted on the membranes from 19th May to 20th May. The plant is operated at a constant 44% recovery from 15th March to 21st April. Thenceforth, the recovery is increased to 49%. During this period, the permeate conductivity has almost doubled due to temperature increase and/or mechanical damage (Fig. 6). However, the permeate flow is not increasing significantly after this period, which rules out mechanical damage as the likely reason.

The NDP is continuously increasing from 0.7 to 2.5 bar. The increase in NDP is a strong indication that the membrane is facing a fouling problem. The NPF is relatively constant at 800 m^3/d from 15th March to 21st April. Hereafter, the NPF is increased to 850 m^3/d. This is in line with the increase in recovery. The NSP from 15th March to 21st April is lower compared to the value after.

3.4. Specific membrane energy consumption

The specific membrane energy consumption is highly affected by the pressure and flowrate. As expected, the fluctuation of feed pressure (Fig. 6A) leads to fluctuation

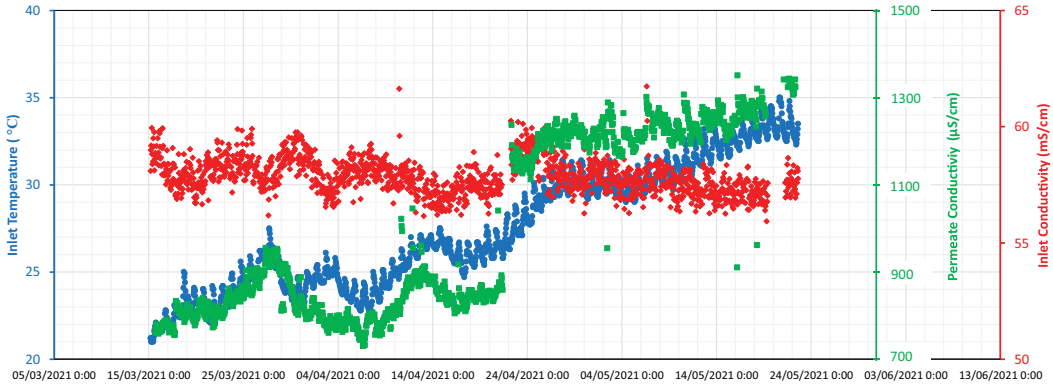

Fig. 5. Operational data for monitoring and diagnosis.

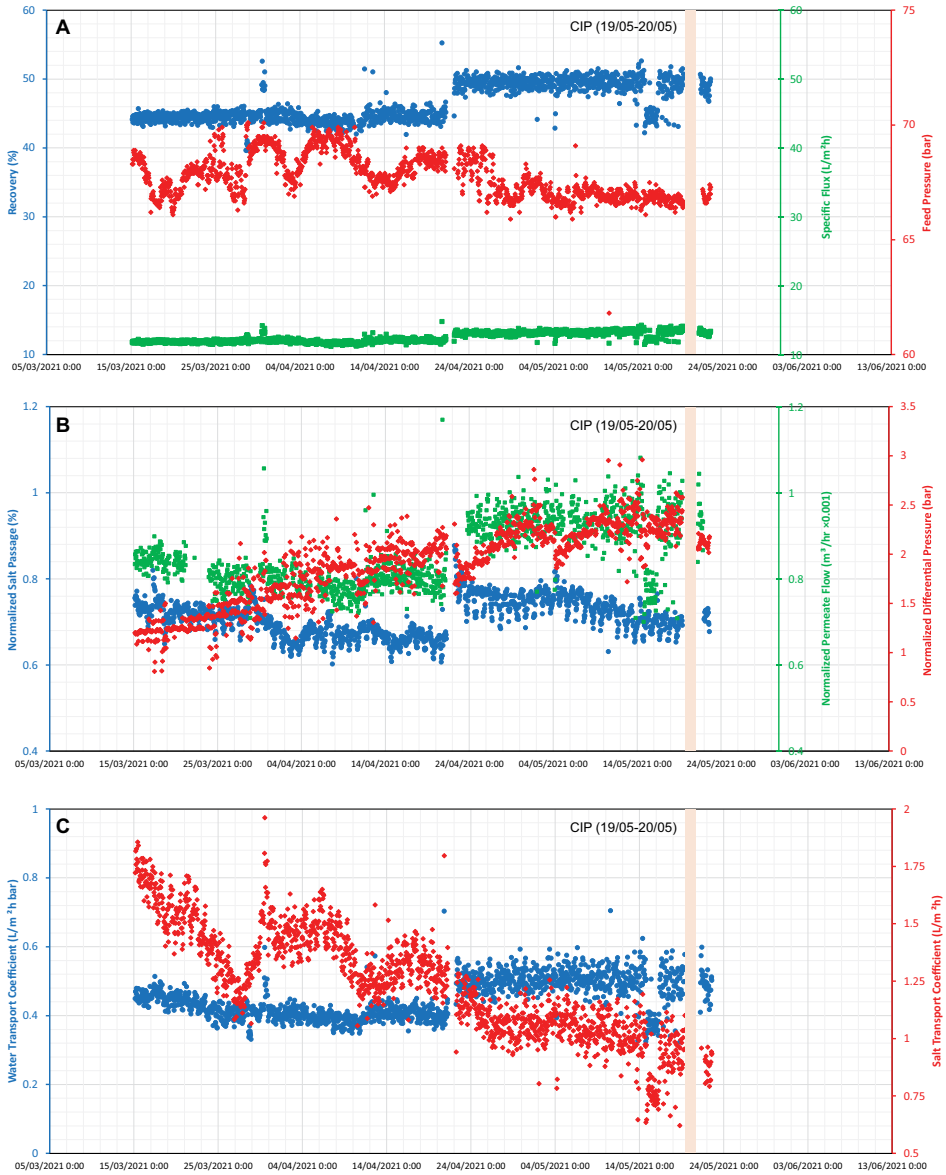

Fig. 6. Data normalization results were obtained from RO-TRACK using the TORAY method. (A) Recovery, feed pressure, specific flux, (B) normalized salt passage, normalized permeate flow, normalized differential pressure, and (C) water transport coefficient, and salt transport coefficient.

of specific membrane energy consumption (Fig. 7), specifically in 15/03/2021 to 24/04/2021. It is also clear that the membrane energy consumption is increasing with the time before CIP. The CIP that is conducted at 19/05/2021 proven to not only lower the normalized differential pressure (Fig. 6B), but also the specific membrane energy consumption. The advantage of this parameter is that we can compare apple-to-apple the specific membrane energy consumption with different trains. In contrast, the normalized data is comparing the membrane with its initial performance. This causes a difficulty for operator to quickly compare the trains performance, therefore, render inefficiency in decision making at the plant.

3.5. CIP prediction and membrane diagnostic

In this section, we present the capability of RO-TRACK to forecast the CIP timeline and provide the root cause of the membrane performance issues. We compare RO-TRACK results with the real-plant condition in a SWRO plant in the United Arab Emirates. From the normalized data, we obtain the trends. The trends are then utilized to identify potential problems that drive the decline in membrane performance. It is to be noted that the data for trend recognition and prediction should be based on operational data without any interruptions and constant operating conditions. Hence, to diagnose and predict the membrane performance, we utilize the data from 15th March to 21st April.

From the qualitative perspective, the selected data of NDP, NPF, and NSP's have increasing, decreasing, and decreasing trend, respectively. This is a strong indication that the membrane performance is declining. By passing this information with the trend of feed pressure, permeate quality, and other water physical properties, to the diagnostic tree, we obtain that the possible cause of the membrane performance decline, organic fouling (NOM), inorganic (metal/colloidal) and/or membrane compaction. We then compare the result with the autopsy result as shown in Table 2.

In addition to the diagnostic, RO-TRACK also predicts the recommended timing for the next CIP. The user will set the maximum allowable NDP and minimum allowable NPF. In this case, we set the NDP for 2.4 bar. Based on the data analysis during this period, the NDP is increasing by 0.2 bar/week. As the CIP decision is mainly driven by NDP to reduce energy consumption in the process, RO-TRACK suggests that the CIP to be conducted on 2nd May. In the real plant operation, prior to reaching the NDP limit, the plant operators tweak the operations by adjusting the feed pressure to maintain the NDP below the limit, the CIP then is delayed until 19th May, which improves operational

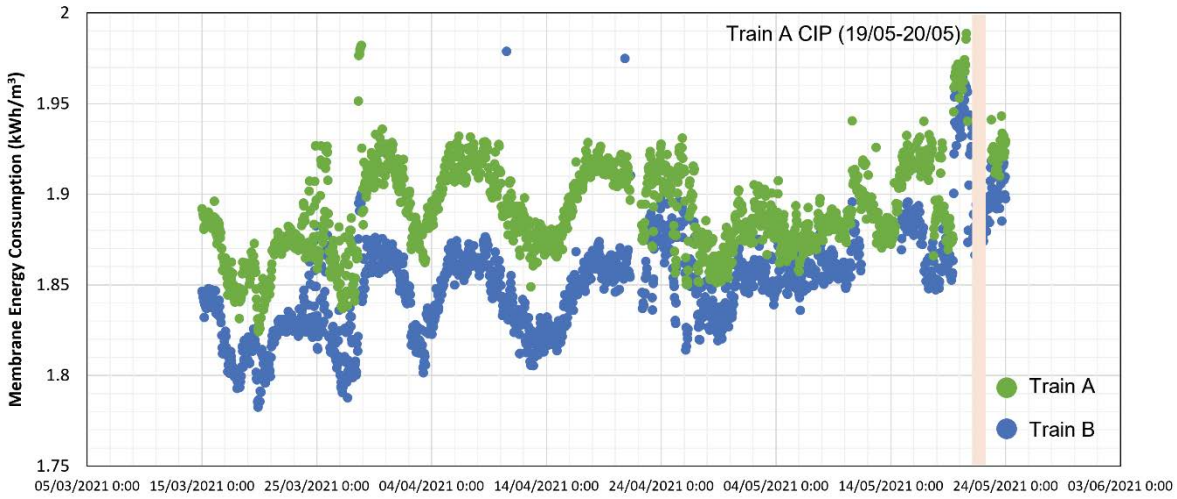

Fig. 7. Specific membrane energy consumption for Trains A and B.

Table 2
Comparison of membrane autopsy result and RO-TRACK diagnostics

RO-TRACK	Membrane autopsy result
Diagnostic result Trend From 2021-03-14 20:00:00 to 2021-05-30 20:00:00: The NDP's trend is increasing. The NPF's trend is decreasing. The NSP's trend is decreasing. The possible cause is organic fouling (NOM), inorganic (metal, colloidal) and/or membrane compaction. Diagnostic The NDP's trend is increasing from 2021-03-14 20:00:00 to 2021-05-30 20:00:00 by the rate of 0.1915584633714526 bar/week. The next CIP is predicted on 2021-05-02 17:03:12.186530.	Autopsy result suggests an increase in organic material (TOC), biofilm development (ATP, total cell count), and accumulation of inorganic material.

resilience and increases plant availability. To corroborate the results of our advanced analytics, we provide more comparison with different plant membrane autopsy results in SI section 9.

The utilization of predictive analytics for monitoring and diagnostic will enable the minimization of membrane replacement. This is achieved by taking proactive steps to prevent irreversible damages on the membranes. With limited number of sensors, prediction in specific membrane to be replaced is non-viable. However, the predictive membrane replacement rate could further be developed. We are currently developing membrane replacement tool to monitor membranes in the train including their average age.

4. Conclusions

In summary, we present the most comprehensive membrane monitoring and diagnostic tool for SWRO desalination plants. The operational data from the plant is sequentially cleaned, validated, and analyzed to obtain such insights. As an output, the program is targeted to provide the plant operators with recommendations on CIP timelines. In addition to that, the diagnosis of the membrane performance decline is provided. The test case of the software is based on one of the trains of the large-scale plant with a production capacity of 225,000 m^3/d. Based on the 5 weeks' operational data, the system provides the operator with the root cause of membrane performance decline and an estimated CIP timeline suggestion based on operational limits. The result is then compared with the real operational experiences and autopsy results. The data-driven insights provide a logical and responsible suggestion to the plant operator. The insights will enable preventive and corrective action ahead of time to prevent irreversible damage to the membrane. To this end, plant availability increases, and the membrane replacement rate reduces. With subsequent use, testing and data training the future version of this software will be able to provide different levels of suggestions such as a differentiation between probable, possible, and proven causes.

CRediT authorship contribution statement

Data collection and Data curation, Thomas Altmann: Writing – Reviewing and Editing Ahmed Yousry: Methodology, Data collection, Writing – review and editing Hussain Basamh: Data curation, Writing – review and editing Ratul Das: Data curation, Conceptualization, Writing – Original draft preparation.

Declaration of competing interest

The authors declare that they have no known competing financial interests or personal relationships that could have appeared to influence the work reported in this paper.

Acknowledgement

The authors would like to thank colleagues from the project companies and NOMAC plant operation team for their support on this project.

References

[1] M. Elimelech, W.A. Phillip, The future of seawater desalination: energy, technology, and the environment, Science, 333 (2011) 712–717.
[2] M.M. Mekonnen, A.Y. Hoekstra, Four billion people facing severe water scarcity, Sci. Adv., 2 (2016) e1500323, doi: 10.1126/sciadv.1500323.
[3] Q. Schiermeier, Water: purification with a pinch of salt, Nature, 452 (2008) 260–261.
[4] M. Qasim, M. Badrelzaman, N.N. Darwish, N.A. Darwish, N. Hilal, Reverse osmosis desalination: a state-of-the-art review, Desalination, 459 (2019) 59–104.
[5] T. Altmann, P.J. Buijs, A.S.F. Farinha, V.R.P. Borges, N.M. Farhat, J.S. Vrouwenvelder, R. Das, Seawater reverse osmosis performance decline caused by short-term elevated feed water temperature, Membranes (Basel), 12 (2022) 792, doi: 10.3390/membranes12080792.
[6] R. Das, S. Arunachalam, Z. Ahmad, E. Manalastas, H. Mishra, Bio-inspired gas-entrapping membranes (GEMs) derived from common water-wet materials for green desalination, Journal of Membrane Science, 588 (2019) 117185, doi: 10.1016/j.memsci.2019.117185.
[7] R. Das, S. Arunachalam, Z. Ahmad, E. Manalastas, A. Syed, U. Buttner, H. Mishra, Proof-of-concept for gas-entrapping membranes derived from water-loving SiO_2/Si/SiO_2 wafers for green desalination, J. Vis. Exp., (2020) e60583, doi: 10.3791/60583.
[8] G. Gonzalez-Gil, A.R. Behzad, A.S.F. Farinha, C. Zhao, S.S. Bucs, P. Buijs, J. Vrouwenvelder, Clinical autopsy of a reverse osmosis membrane module, Front. Chem. Eng., 3 (2021) 23, doi: 10.3389/fceng.2021.683379.
[9] M.A. Shannon, P.W. Bohn, M. Elimelech, J.G. Georgiadis, B.J. Mariñas, A.M. Mayes, Science and technology for water purification in the coming decades, Nature, 452 (2008) 301–310.
[10] G. Hasanin, A.M. Mosquera, A.-H. Emwas, T. Altmann, R. Das, P.J. Buijs, J.S. Vrouwenvelder, G. Gonzalez-Gil, The microbial growth potential of antiscalants used in seawater desalination, Water Res., 233 (2023) 119802, doi: 10.1016/j.watres.2023.119802.
[11] L. Wang, C. Violet, R.M. DuChanois, M. Elimelech, Derivation of the theoretical minimum energy of separation of desalination processes, J. Chem. Educ., 97 (2020) 4361–4369.
[12] J.R. Werber, M. Elimelech, Permselectivity limits of biomimetic desalination membranes, Sci. Adv., 4 (2018), doi: 10.1126/sciadv.aar8266.
[13] H.B. Park, J. Kamcev, L.M. Robeson, M. Elimelech, B.D. Freeman, Maximizing the right stuff: the trade-off between membrane permeability and selectivity, Science, 356 (2017) eaab0530, doi: 10.1126/science.aab0530.
[14] S.S. Shenvi, A.M. Isloor, A.F. Ismail, A review on RO membrane technology: developments and challenges, Desalination, 368 (2015) 10–26.
[15] T. Altmann, A. Rousseva, J. Vrouwenvelder, M. Shaw, R. Das, Effectiveness of ceramic ultrafiltration as pretreatment for seawater reverse osmosis, Desalination, 564 (2023) 116781, doi: 10.1016/j.desal.2023.116781.
[16] S.K. Al-Mashharawi, N. Ghaffour, M. Al-Ghamdi, G.L. Amy, Evaluating the efficiency of different microfiltration and ultrafiltration membranes used as pretreatment for Red Sea water reverse osmosis desalination, Desal. Water Treat., 51 (2013) 617–626.
[17] T.M. Missimer, N. Ghaffour, A.H.A. Dehwah, R. Rachman, R.G. Maliva, G. Amy, Subsurface intakes for seawater reverse osmosis facilities: capacity limitation, water quality improvement, and economics, Desalination, 322 (2013) 37–51.
[18] J.L. Pearson, P.R. Michael, N. Ghaffour, T.M. Missimer, Economics and energy consumption of brackish water reverse osmosis desalination: innovations and impacts of feedwater quality, Membranes, 11 (2021) 616, doi: 10.3390/membranes11080616.
[19] Global Water Intelligence, Searching for Substance in the Digital Twin Market, 2022.

[20] M.G. Ridwan, T. Altmann, A. Yousry, R. Das, Intelligent framework for coagulant dosing optimization in an industrial-scale seawater reverse osmosis desalination plant, Mach. Learn. Appl., 12 (2023) 100475, doi: 10.1016/j.mlwa.2023.100475.
[21] M. Aghaei, F. Grimaccia, C.A. Gonano, S. Leva, Innovative automated control system for PV fields inspection and remote control, IEEE Trans. Ind. Electron., 62 (2015) 7287–7296.
[22] K. Sayed, H.A. Gabbar, Chapter 18 – SCADA and Smart Energy Grid Control Automation, H.A. Gabbar, Ed., Smart Energy Grid Engineering, Elsevier, 2017, pp. 481–514.
[23] S. Al Aani, T. Bonny, S.W. Hasan, N. Hilal, Can machine language and artificial intelligence revolutionize process automation for water treatment and desalination?, Desalination, 458 (2019) 84–96.
[24] J. Leparc, S. Rapenne, C. Courties, P. Lebaron, J.P. Croué, V. Jacquemet, G. Turner, Water quality and performance evaluation at seawater reverse osmosis plants through the use of advanced analytical tools, Desalination, 203 (2007) 243–255.
[25] A. Yousry, M.G. Ridwan, T. Altmann, A. Rousseva, K. Azab, R. Das, Performance model for reverse osmosis, Chem. Eng. Res. Des., 186 (2022) 416–432.
[26] K.O. Agenson, T. Urase, Change in membrane performance due to organic fouling in nanofiltration (NF)/reverse osmosis (RO) applications, Sep. Purif. Technol., 55 (2007) 147–156.
[27] A. Ruiz-García, N. Melián-Martel, I. Nuez, Short review on predicting fouling in RO desalination, Membranes, 7 (2017) 62, doi: 10.3390/membranes7040062.
[28] M. Adel, T. Nada, S. Amin, T. Anwar, A.A. Mohamed, Characterization of fouling for a full-scale seawater reverse osmosis plant on the Mediterranean sea: membrane autopsy and chemical cleaning efficiency, Groundwater Sustainable Dev., 16 (2022) 100704, doi: 10.1016/j.gsd.2021.100704.
[29] M. Amin Saad, Early discovery of RO membrane fouling and real-time monitoring of plant performance for optimizing cost of water, Desalination, 165 (2004) 183–191.
[30] A.J. Karabelas, S.T. Mitrouli, M. Kostoglou, Scaling in reverse osmosis desalination plants: a perspective focusing on development of comprehensive simulation tools, Desalination, 474 (2020) 114193, doi: 10.1016/j.desal.2019.114193.
[31] H. Huiting, J.W.N.M. Kappelhof, T.G.J. Bosklopper, Operation of NF/RO plants: from reactive to proactive, Desalination, 139 (2001) 183–189.
[32] M. Safar, M. Jafar, M. Abdel-Jawad, S. Bou-Hamad, Standardization of RO membrane performance, Desalination, 118 (1998) 13–21.
[33] T.Y. Cath, M. Elimelech, J.R. McCutcheon, R.L. McGinnis, A. Achilli, D. Anastasio, A.R. Brady, A.E. Childress, I.V. Farr, N.T. Hancock, J. Lampi, L.D. Nghiem, M. Xie, N.Y. Yip, Standard methodology for evaluating membrane performance in osmotically driven membrane processes, Desalination, 312 (2013) 31–38.
[34] A.H. Nguyen, J.E. Tobiason, K.J. Howe, Fouling indices for low pressure hollow fiber membrane performance assessment, Water Res., 45 (2011) 2627–2637.
[35] I. TORAY Industries, TORAY TRAK™, 2022.
[36] ASTM Materials, Standard Practice for Standardizing Reverse Osmosis Performance Data, ASTM (American Society for Testing and Materials), 2000.
[37] M.G. Kendall, A new measure of rank correlation, Biometrika, 30 (1938) 81–93.
[38] R.M. Hirsch, J.R. Slack, A nonparametric trend test for seasonal data with serial dependence, Water Resour. Res., 20 (1984) 727–732.

Supporting information

S1. Common normalization calculation

Data normalization contains intermediate calculations of main parameters that are used in all methods such as: days of operation, feed flow, differential pressure, net driving pressure, recovery, actual salt passage, actual salt rejection, and normalized permeate flow. This section defines common parameters that are used in intermediate calculations for all data standardization approaches. Days of operation is calculated for each set of inputs to show the total number of days during which the plant has been operating up to inputs date. It can be calculated using start-up date of the plant and date of certain readings as shown in Eq. (S1):

$$\text{Days of Operation} = \text{Date}_{\text{Reading}} - \text{Date}_{\text{Start}} \tag{S1}$$

where $\text{Date}_{\text{Reading}}$ is date at which measurements are collected and start-up date is the first operating day of the plant. Feed flow at any point is calculated as sum of concentrate and permeate flowrates at that point as shown in Eq. (S2):

$$Q_F\left(\text{m}^3/\text{h}\right) = Q_C\left(\text{m}^3/\text{h}\right) + Q_P\left(\text{m}^3/\text{h}\right) \tag{S2}$$

where concentrate and permeate flowrates are inputs in each set of measurements. Differential pressure (DP) is also calculated using inputted readings as shown in Eq. (S3):

$$\text{DP}\left(\text{bar}\right) = P_F\left(\text{bar}\right) - P_C\left(\text{bar}\right) \tag{S3}$$

where feed and concentrate pressure are direct inputs for each set of data. Recovery (Y) can be also calculated using permeate and feed flowrates as shown in Eq. (S4):

$$Y\left(\%\right) = \frac{Q_P\left(\text{m}^3/\text{h}\right)}{Q_F\left(\text{m}^3/\text{h}\right)} \times 100 \tag{S4}$$

where permeate flow (m^3/h) is a direct input for each set of inputs, and feed flow (m^3/h) is calculated for each set of data as shown in Eq. (S4). Generally, salt passage (SP) and salt rejection (SR) are two parameters that can be calculated in reverse osmosis (RO) systems as shown in Eq. (S5):

$$\text{SP}\left(\%\right) = \frac{C_P\left(\text{mg/L}\right)}{C_F\left(\text{mg/L}\right)} \times 100 \tag{S5}$$

where C_P (permeate total dissolved solids (TDS; mg/L)) and C_F (feed TDS (mg/L)) are calculated as a function of electrical conductivity for each set of daily inputs. Electrical conductivity to TDS conversion has different correlations developed by different membrane vendors. Therefore, usage of the right correlation for the relevant approach is necessary. Salt rejection (%) can then be calculated using salt passage (%) as shown in Eq. (S6):

$$\text{SR}\left(\%\right) = 100 - \text{SP}\left(\%\right) \tag{S6}$$

Net driving pressure (NetDP) is an important term in data normalization that refers to the measure of the actual driving pressure available to force water through the RO membranes. Normalized differential pressure (NDP) is calculated for both reference conditions (initial at $t = 0$ or specified) and operating conditions (actual at time = t) the same way in all methods as shown in Eq. (S7):

$$\text{NetDP}\left(\text{bar}\right) = P_F - \frac{\text{DP}}{2} - P_P - \pi_{\text{FC}} + \pi_P \tag{S7}$$

where P_F is the feed pressure inserted in bar for each set of inputs, DP is the differential pressure calculated in bar as shown in Eq. (S7), P_P is the permeate pressure inputted in bar for each set of inputs, π_{FC} and π_P are the calculated feed-brine osmotic pressure (bar) and the calculated permeate osmotic pressure (bar), respectively. Osmotic pressures can be calculated using different correlations, each approach below has its own way to calculate osmotic pressures. In some approaches such as: DuPont (DuPont document), due to the low value of permeate osmotic pressure π_P in data normalization, it is considered negligible and is not added to the NDP equation in normalized permeate flow. However, DuPont considers π_P in NDP used for normalized permeate TDS. Normalized permeate flow (m^3/h) is the first common "Normalized" term among all approaches. It is calculated the same way in all approaches as shown in Eq. (S8):

$$Q_{P,n}\left(\text{m}^3/\text{h}\right) = Q_{P,t}\left(\text{m}^3/\text{h}\right) \times \frac{\text{NDP}_r\left(\text{bar}\right) \times \text{TCF}_r}{\text{NDP}_t\left(\text{bar}\right) \times \text{TCF}_t} \tag{S8}$$

where $Q_{P,t}$ is permeate flowrate at any time (inputted by the user on a daily basis), NDP_r is NDP at reference conditions (initial or standard) calculated as shown in Eq. (S8), NDP_t is NDP at any time = t, TCF_r and TCF_t are temperature correction factors at reference conditions and at any time = t, respectively. Temperature correction factor (TCF) is calculated at certain set of conditions using different correlations and is described for each membrane supplier in the following sections. Water transport coefficient and salt transport coefficient are calculated using:

$$\text{WTC}_n = \frac{Q_{P,n}}{\text{Membrance area} \times \text{total of the membrance} \times 3600 \times \text{NDP} \times 100 \times \text{TCF}}$$

$$\text{STC}_n = \frac{Q_{P,n}}{\text{Membrance area} \times \text{total of the membrance} \times 3600 \times \frac{\text{SP}a}{1-\text{SP}a} \times \text{TCF}}$$

Specific flux (water permeability) can be calculated in $L/(m^2 \cdot h \cdot bar)$ at any point in data normalization as shown in Eq. (S9):

$$\text{Specific Flux}\left(\frac{\text{LMH}}{\text{bar}}\right) = \frac{Q_{P,t}\left(\text{m}^3/\text{h}\right)}{\text{Area}_{\text{Total}}\left(\text{m}^2\right)} \tag{S9}$$

where total area is calculated as $A_{\text{Total}}(\text{m}^2) = A_{\text{Element}}(\text{m}^2) \times N_{\text{Stage}}$.

S2. Details of TORAY normalization method

Permeate and feed-brine osmotic pressures used in NDP are calculated as shown in Eqs. (S10) and (S11):

$$\pi_P\left(\text{bar}\right) = \frac{1.01327 \times 0.082054 \times \left(T + 273.15\right) \times 2 \times 1000 \times 2 \times C_P}{1000 \times 58.44 \times 2 \times 1000} \times \left(10^{\frac{-0.5 \times \sqrt{\frac{1 \times C_P \times 2 \times 1000 \times 1^2 \times 4}{2 \times 2 \times 1000 \times 1000 \times 58.44 \times 2}}}{1 + \sqrt{\frac{1 \times C_P \times 2 \times 1000 \times 1^2 \times 4}{2 \times 2 \times 1000 \times 1000 \times 58.44 \times 2}}}}\right)^{0.14} \tag{S10}$$

Similarly,

$$\pi_{\text{FC}}\left(\text{bar}\right) = \frac{1.01327 \times 0.082054 \times \left(T + 273.15\right) \times 2 \times 1000 \times 2 \times C_{\text{FC}}}{1000 \times 58.44 \times 2 \times 1000} \times \left(10^{\frac{-0.5 \times \sqrt{\frac{1 \times C_{\text{FC}} \times 2 \times 1000 \times 1^2 \times 4}{2 \times 2 \times 1000 \times 1000 \times 58.44 \times 2}}}{1 + \sqrt{\frac{1 \times C_{\text{FC}} \times 2 \times 1000 \times 1^2 \times 4}{2 \times 2 \times 1000 \times 1000 \times 58.44 \times 2}}}}\right)^{0.14} \tag{S11}$$

where T is inputted temperature in °C on a daily basis, C_P is the permeate TDS (mg/L) calculated using energy consumption (EC)-TDS conversion, and C_{FC} (mg/L) is feed-brine average concentration calculated as shown in Eq. (S12):

$$C_{\text{FC}} = C_F \times \frac{1 - \left(1 - Y\right)^{\left(1-\text{SR}\right)}}{\left(1 - \text{SR}\right) \times Y} \tag{S12}$$

where Y and SR are fractions that represent nominal recovery, $Y = Q_P/Q_F$, and nominal salt rejection at time (t), $\text{SR} = 1 - C_P/C_F$. Here, Q_P and Q_F are permeate flowrate and feed flowrate, respectively. Similarly, C_P and C_F represent permeate TDS (mg/L) and feed TDS (mg/L), respectively. C_P and C_F are calculated in mg/L using the same correlation and coefficients. If EC (μS/cm) is greater than 7,630 (EC > 7,630), then $C = uSa \times e^{\frac{\left(uSb - \ln\left(e^{\left(0.0017 \times \left(T-25\right)\right)} \times \text{EC}\right)\right)^2}{uSc}}$, and if EC (μS/cm) is less than 7,630 (EC < 7,630), then $C = uS2a \times e^{\frac{\left(uS2b - \ln\left(e^{\left(0.0017 \times \left(T-25\right)\right)} \times \text{EC}\right)\right)^2}{uS2c}}$, where C is the concentration in mg/L (feed or permeate), and EC is the electrical conductivity in μS/cm (feed or permeate) inputted daily. Table S1 shows coefficients used for EC to TDS conversion.

Temperature correction factor (TCF) used for normalized permeate flow (NPF) is calculated depending on the temperature. If temperature is less than or equal to 25°C ($T \le 25$), then $\text{TCF}_{\text{Flow}} = \mu \times e^{\text{Temp}A1 \times \left(T-25\right)} \times \left(\frac{T_K}{298}\right)^{\frac{\text{Temp}A3}{1-Y}}$, and if temperature is greater than 25°C ($T > 25$), then $\text{TCF}_{\text{Flow}} = \mu \times e^{\text{Temp}A2 \times \left(T-25\right)} \times \left(\frac{T_K}{298}\right)^{\frac{\text{Temp}A4}{1-Y}}$, where Y is the nominal recovery, and μ is water viscosity (factor) calculated as shown in Eq. (S13):

Table S1
EC-TDS conversion coefficients

Coefficient	Value
uSa	0.000000000080090966
uSb	–50.645805186
uSc	112.483950289
uS2a	7.7013840097E-20
uS2b	–90.475562243
uS2c	188.88442227

$$\mu = \frac{e^{\frac{1965}{298.15}}}{e^{\frac{1965}{T_K}}} \tag{S13}$$

where T_K is the temperature in Kelvin. TempA1, TempA2, TempA3 and TempA4 are membrane model related parameters for all TORAY membranes. SP_t is the actual salt passage calculated as show in Eq. (S14):

$$SP_t = \frac{C_{P,t}\left(\text{mg/L}\right)}{CF_{\text{lm},t}\left(\text{mg/L}\right)} \tag{S14}$$

where C_P is the calculated permeate TDS (mg/L) as described in Eq. (S14), and CF_{lm} is the feed-brine average log mean calculated at any time ($t = t/t = 0$) as shown in Eq. (S15):

$$CF_{\text{lm}} = \frac{C_C\left(\text{mg/L}\right) - C_F\left(\text{mg/L}\right)}{\ln\left(\frac{C_C\left(\text{mg/L}\right)}{C_F\left(\text{mg/L}\right)}\right)} \tag{S15}$$

where C_F is the calculated feed TDS described in Eq. (S15), and C_C is the concentrate TDS calculated using mass balance as shown in Eq. (S16):

$$C_C = \frac{C_F Q_F - C_P Q_P}{Q_C} \tag{S16}$$

where C represents concentrations at any time ($t = t/t = 0$), and Q describes flowrate of feed, brine and permeate. TCF_{Salt} is the temperature correction factor used for both normalized salt passage equations (different than TCF_{Flow}) and is calculated as $TCF_{Salt} = \frac{\mu_{25}}{\mu_T} \times e^{\text{TempB1}\times(T-25)} \times \left(\frac{T_K}{298}\right)^{\frac{\text{TempB3}}{1-Y}}$ for $T \le 25$, and $TCF_{Salt} = \frac{\mu_{25}}{\mu_T} \times e^{\text{TempB2}\times(T-25)} \times \left(\frac{T_K}{298}\right)^{\frac{\text{TempB4}}{1-Y}}$ for $T > 25$, where T_K and Y are temperature in K and nominal recovery described in Eq. (S16). TempB1, TempB2, TempB3, TempB4 are membrane model related parameters for all TORAY membranes. μ_{25} and μ_T are feed-brine average viscosities at temperature 25°C and at temperature T (daily input), respectively. Feed-brine average viscosity at 25°C can be calculated as shown in Eq. (S17):

$$\mu_{25} = 1.234\times10^{-6}\times e^{\frac{0.00212\times CF_{\text{lm}}\times\rho_{25}}{1000\times1000}+\frac{1965}{273.15+25}} \tag{S17}$$

where CF_{lm} is feed-brine average log mean described in Eq. (S17), and ρ_{25} (kg/m^3) is feed-brine average density at 25°C calculated as shown in Eq. (S18):

$$\rho_{25} = \frac{1000\times\left(1+\frac{0.00714\times CF_{\text{lm}}}{10000}\right)}{\begin{aligned}&3.1975+\left(-0.315154\times\left(\left(647.27-\left(25+273.15\right)\right)^{1/3}\right)\right)\\&+\left(-0.001203374\times\left(647.27-\left(25+273.15\right)\right)\right)\\&+\left(0.000000000000748908\times\left(647.27-\left(25+273.15\right)\right)^4\right)\\&\frac{}{1+\left(0.1342489\times\left(647.27-\left(25+273.15\right)\right)^{1/3}\right)}\\&+\left(-0.003946263\times\left(647.27-\left(25+273.15\right)\right)\right)\end{aligned}} \tag{S18}$$

Similarly, feed-brine average viscosity at temperature T is calculated as shown in Eq. (S19):

$$\mu_T = 1.234\times10^{-6}\times e^{\frac{0.00212\times CF_{\text{lm}}\times\rho_T}{1000\times1000}+\frac{1965}{273.15+T}} \tag{S19}$$

where ρ_T (kg/m^3) is calculated as shown in Eq. (S20):

$$\rho_{25} = \frac{1000\times\left(1+\frac{0.00714\times CF_{\text{lm}}}{10000}\right)}{\begin{aligned}&3.1975+\left(-0.315154\times\left(\left(647.27-\left(T+273.15\right)\right)^{1/3}\right)\right)\\&+\left(-0.001203374\times\left(647.27-\left(T+273.15\right)\right)\right)\\&+\left(0.000000000000748908\times\left(647.27-\left(T+273.15\right)\right)^4\right)\\&\frac{}{1+\left(0.1342489\times\left(647.27-\left(T+273.15\right)\right)^{1/3}\right)}\\&+\left(-0.003946263\times\left(647.27-\left(T+273.15\right)\right)\right)\end{aligned}} \tag{S20}$$

where CF_{lm} is the feed-brine average log mean described in Eq. (S20), and T is the daily measured temperature. The third normalized term by TORAY is the normalized differential pressure, which is calculated as shown in Eq. (S21):

$$NDP\left(\text{bar}\right) = DP_t\left(\text{bar}\right)\times\left(\frac{Q_{\text{FC},0}}{Q_{\text{FC},t}}\right)^{\text{DeltaP3}}\times\left(\frac{\mu_{T,0}}{\mu_{T,t}}\right)^{\text{DeltaP6}} \tag{S21}$$

where DP is differential pressure calculated in previous section ($P_F - P_C$), μ_T is the feed brine average viscosity shown in Eq. (S21), and Q_{FC} is the feed brine average flow calculated at any time ($t = t/t = 0$) as shown here, $Q_{\text{FC}}\left(\text{m}^3/\text{h}\right) = \frac{Q_F\left(\text{m}^3/\text{h}\right)+Q_C\left(\text{m}^3/\text{h}\right)}{2}$, where Q_F and Q_C are feed and concentrate flowrate describes previously. DeltaP3 and DeltaP6 are membrane model related parameters for all TORAY membranes.

S3. Details of ASTM normalization method

Further, American Society for Testing and Materials (ASTM) practice covers the standardization of permeate flow, salt passage, and coefficient of performance of RO systems at a standard set of conditions using data obtained at actual operating conditions. Normalized permeate flow is calculated using TCF and NDP. TCF at any time ($t = t/t = 0$) is calculated as shown in Eq. (S22):

$$\mathrm{TCF} = 1.03^{T-25} \tag{S22}$$

where T is temperature in °C. Feed-brine osmotic pressure is calculated as shown in Eq. (S23):

$$\pi_{\mathrm{FC}}\left(\mathrm{bar}\right) = \frac{0.2654 \times C_{\mathrm{FC}} \times \left(T + 273.15\right)}{\left(1000 - \left(\frac{C_{\mathrm{FC}}}{1000}\right)\right) \times 100} \tag{S23}$$

where C_{FC} is feed-brine average concentration calculated using one of the Eqs. (S24) and (S25):

$$C_{\mathrm{FC}}\left(\mathrm{mg/L\ as\ NaCl}\right) = C_F \times \frac{\ln\left(\frac{1}{1-Y}\right)}{Y} \tag{S24}$$

$$C_{\mathrm{FC}}\left(\mathrm{mg/L\ as\ NaCl}\right) = \frac{C_F + C_C}{2} \tag{S25}$$

where C_C is brine concentration in mg/L as NaCl, C_F is feed concentration in mg/L as NaCl, and Y is nominal recovery (Q_P/Q_F). Permeate osmotic pressure is calculated as shown as π_P (bar) = 0.01 × π_{FC} (bar), EPF_r and EPF_a are the average element permeate flow at reference (standard or initial) and at actual conditions, respectively. EPF is permeate flow (reference or actual) of the RO system divided by the number of membrane elements operating in the system as shown in Eq. (S26):

$$\mathrm{EPF} = \frac{Q_p\left(\mathrm{m^3/h}\right)}{\text{Total No. of Elements}} \tag{S26}$$

where total number of elements in the system is calculated as shown in Eq. (S27):

$$\begin{aligned}\text{Total No. of Elements} = {} & \text{No. of Elements per PV} \\ & \times \text{No. PVs per Stage}\end{aligned} \tag{S27}$$

STCF is salt transport temperature correction factor which is dependent on the membrane type material and configuration. STCF equations shall be obtained from manufacturer, if unavailable then TCF can be applied. SP_t is the actual salt passage calculated as shown in Eq. (S28):

$$\mathrm{SP}_t = \frac{C_P}{C_F} \tag{S28}$$

It is important to know that ASTM approach uses concentration as mg·NaCl/L. In order to get concentration of feed (C_F) as mg/L as NaCl, osmotic pressure of RO feed shall be calculated using Eq. (S29):

$$\pi_F\left(kPa\right) = 8.308 \times \varnothing \times \left(T_F + 273.15\right) \times \sum m_i \tag{S29}$$

where $\varnothing$ is the osmotic coefficient, $\sum m_i$ is the sum of molalities of all ionic and non-ionic constituents in seawater. This equation requires a detailed ion composition of all ions present in seawater to estimate sum of molalites and osmotic coefficient. ASTM estimates osmotic coefficient value for seawater to be 0.90. Feed concentration (C_F) can then be calculated as shown in Eq. (S30):

$$C_F\left(\mathrm{mg/L\ as\ NaCl}\right) = \frac{1000 \times \pi_F\left(kPa\right)}{0.2654 \times \left(T_F + 273.15\right) + \frac{\pi_F\left(kPa\right)}{1000}} \tag{S30}$$

where T_F is the feed stream temperature in °C. C_F in mg/L as NaCl is the basis for all calculations in ASTM method if the first C_{FC} equation is used. In case the second C_{FC} equation applies, then C_C (concentration of brine as mg/L as NaCl) is calculated as shown in Eq. (S31):

$$C_C\left(\mathrm{mg/L\ as\ NaCl}\right) = \frac{C_F\left(\mathrm{mg/L\ as\ NaCl}\right)}{1-Y} \tag{S31}$$

where Y is recovery expressed as decimal (fraction).

S4. Details of DOW normalization method

Normalized terms from DOW include normalized permeate flow and normalized salt passage. As described earlier, NDP and normalized permeate flow are common calculations for all approaches. DOW has different correlation for TCF and osmotic pressures. TCF used for normalized permeate flow is calculated as shown in Eq. (S32):

$$\mathrm{TCF} = 2640 \times \left(\frac{1}{298.15} - \frac{1}{T + 273.15}\right) \tag{S32}$$

where T is daily measured temperature in °C. Feed-brine and permeate osmotic pressures used for NDP calculation are estimated as shown in Eqs. (S33) and (S34):

$$\pi_{\mathrm{FC}}\left(\mathrm{bar}\right) = \frac{0.0385 \times C_{\mathrm{FC}} \times \left(T + 273.15\right)}{\left(1000 - \left(\frac{C_{\mathrm{FC}}}{1000}\right)\right) \times 14.5} \tag{S33}$$

$$\pi_P\left(\mathrm{bar}\right) = \frac{0.0385 \times C_P \times \left(T + 273.15\right)}{\left(1000 - \left(\frac{C_P}{1000}\right)\right) \times 14.5} \tag{S34}$$

where C_P is permeate TDS (mg/L) explained later. C_{FC} is feed-brine average concentration and is calculated in mg/L as shown in Eq. (S35):

$$C_{\mathrm{FC}}\left(\mathrm{mg/L}\right) = C_F \times \frac{\ln\left(1 \Big/ \left(1 - \frac{Q_P}{Q_F}\right)\right)}{Q_P / Q_F} \tag{S35}$$

Table S2
EC-TDS conversion factors

Coefficient	Value
a1	0.000000000080090966
b1	–50.645805186
c1	112.483950289
a2	7.7013840097E-20
b2	–90.475562243
c2	188.88442227

where Q_P and Q_F are permeate and feed flowrates (Note: Q_P/Q_F = recovery, Y), respectively. Feed TDS (C_F) and permeate TDS (C_P) are calculated in mg/L using electrical conductivities as $C\left(\text{mg/L}\right)=a1\times e^{\frac{\left(b1-\ln\left(\text{EC}\right)\right)^2}{c1}}$ for EC (μS/cm) > 7,630 and $C\left(\text{mg/L}\right)=a2\times e^{\frac{\left(b2-\ln\left(\text{EC}\right)\right)^2}{c2}}$ for EC (μS/cm) ≤ 7,630, where C is concentration of feed or permeate in mg/L. Correction factors used in Eq. (S35) are as shown in Table S2. where EC is electrical conductivity measured daily in μS/cm. The second normalized term is normalized salt passage, which is calculated as shown in Eq. (S36):

$$\text{SP}_n=\frac{C_{P,t}}{C_{F,t}}\times\frac{Q_{p,t}\times\text{TCF}_0\times C_{\text{FC},0}\times C_{F,t}}{Q_{p,t}\times\text{TCF}_t\times C_{\text{FC},t}\times C_{F,0}} \tag{S36}$$

where subscript t represents calculation at any time = t, and subscript 0 is for t = 0 calculations. Normalized salt rejection can then be calculated as shown in Eq. (S37):

$$\text{SR}_n=1-\text{SP}_n \tag{S37}$$

where SP_n is normalized salt passage as a fraction. Further actual salt passage is defined as:

$$\text{SPa}=\frac{C_{P,t}}{C_{\text{FC}}} \tag{S38}$$

S5. Details of DuPont normalization method

DuPont approach is almost the same as DOW method. However, few discrepancies were recognized between both methods such as: TCF and osmotic pressure correlations. Temperature correction factor is calculated in DuPont (DuPont Document) as expressed, $\text{TCF}=2640\times\left(\frac{1}{298.15}-\frac{1}{T+273.15}\right)$ for T ≥ 25°C, and $\text{TCF}=3020\times\left(\frac{1}{298.15}-\frac{1}{T+273.15}\right)$ for T < 25°C, where T is daily measured temperature. Feed-brine osmotic pressure is calculated as $\pi_{\text{FC}}\left(\text{bar}\right)=\frac{C_{\text{FC}}\times\left(T+320\right)}{491000}$ for C_{FC} (mg/L) < 20,000, and $\pi_{\text{FC}}\left(\text{bar}\right)=\frac{0.0117C_{\text{FC}}-34}{14.23}\times\frac{T+320}{345}$ for C_{FC} (mg/L) > 20,000, where T is measured temperature in °C, and C_{FC} is feed-brine average concentration calculated similar to DOW using C_F and recovery Y (Q_P/Q_F).

DuPont normalizes mainly permeate flow and permeate TDS. Normalized permeate flow is calculated using the same common equation described earlier. However, permeate osmotic pressure is negligible in NDP calculation for normalized permeate flow. Normalized permeate TDS is calculated as shown in Eq. (S39):

$$C_{P,n}\left(\text{mg/L}\right)=C_{P,t}\times\frac{P_{F,t}-\frac{\text{DP}_t}{2}P_{p,t}-\pi_{\text{FC},t}+\pi_{P,t}}{P_{F,0}-\frac{\text{DP}_0}{2}P_{p,0}-\pi_{\text{FC},\mathbf{0}}+\pi_{P,0}}\times\frac{C_{\text{FC},0}}{C_{\text{FC},t}} \tag{S39}$$

where $C_{P,t}$ is permeate TDS at time = t. Normalized salt rejection can then be calculated as expressed in Eq. (S40):

$$\text{SR}_n=1-\frac{C_{P,n}}{C_{F,0}} \tag{S40}$$

Then, normalized salt passage is defined as SP_n = 1–SR_n and actual salt passage is defined as SPa = $C_{P,t}/C_{\text{FC}}$. Permeate osmotic pressure is unavailable. It can be assumed that permeate osmotic pressure is 0 bar.

S6. Details of LG normalization method

The majority of calculations in LG data normalization are similar to what is explained earlier. However, LG calculations contain new defined parameters such as B correction and polarization factors. Moreover, TCF and permeate osmotic pressure are different than previous methods. LG normalization terms consist of permeate flow, salt passage, salt rejection and permeate TDS. Normalized permeate flow is calculated using the same common equation where TCF is calculated as shown in Eq. (S41):

$$\text{TCF}=3070\times\left(\frac{1}{298.15}-\frac{1}{T+273.15}\right) \tag{S41}$$

where T is daily measured temperature in °C. Feed-brine and permeate osmotic pressures used for NDP calculations are estimated as expressed in Eq. (S42):

$$\pi_{\text{FC}}\left(\text{bar}\right)=\frac{0.0385\times C_{\text{FC}}\times\left(T+273.15\right)}{\left(1000-\left(\frac{C_{\text{FC}}}{1000}\right)\right)\times 14.5} \tag{S42}$$

where feed-brine average concentration C_{FC} is calculated as shown in Eq. (S43):

$$C_{\text{FC}}\left(\text{mg/L}\right)=C_F\times\text{Polarization}\times\frac{-\ln\left(1-Y\right)}{Y} \tag{S43}$$

where polarization factor is calculated as described as $\text{Polarization}=\left(e^{\frac{0.75\times 2\times Y}{2-Y}}\right)^{1/8}$ where Y is the recovery calculated as $Y=\frac{Q_P\left(\text{m}^3/\text{h}\right)}{Q_F\left(\text{m}^3/\text{h}\right)}$. C_F and C_P are calculated using electrical conductivities (μS/cm) as shown in Eq. (S44):

$$C\left(\text{mg/L}\right)=\left(2.0282\times10^{-6}\times\text{EC}^{2}\right)+\left(0.522\times\text{EC}\right) \tag{S44}$$

where C is concentration (TDS) of feed or permeate in mg/L. Permeate osmotic pressure can be calculated as shown in Eq. (S45):

$$\pi_{P}\left(\text{bar}\right)=\frac{1.8\times\frac{C_{P}}{55850}\times0.0821\times\left(T+273\right)\times14.7}{14.504} \tag{S45}$$

where C_P (mg/L) is permeate TDS calculated in Eq. (S45), and T is daily recorded temperature in °C. The second normalized term is the salt passage, which is calculated as shown in Eq. (S46):

$$\text{SP}_{n}=\frac{C_{P,t}}{C_{F,t}}\times\frac{Q_{P,t}\times\text{TCF}_{0}\times C_{\text{FC},0}\times C_{F,t}\times B_{0}}{Q_{P,0}\times\text{TCF}_{t}\times C_{\text{FC},t}\times C_{F,0}\times B_{t}} \tag{S46}$$

where B is a correction factor calculated as shown in Eq. (S47):

$$B=5030\times\left(\frac{1}{298.15}+\frac{1}{T+273.15}\right) \tag{S47}$$

where T is daily measured temperature in °C. Normalized salt rejection can then be calculated as SR_n = 1–SP_n. Normalized permeate TDS is calculated as shown in Eq. (S48):

$$C_{P,n}\left(\text{mg/L}\right)=\left(1-\text{SR}_{n}\right)\times C_{F,0} \tag{S48}$$

where $C_{F,0}$ is the feed TDS calculated at t = 0. Further actual salt passage is defined as SPa = $C_{P,t}/C_{\text{FC}}$.

S7. Details of Hydranautics normalization method

In addition to permeate flow and salt passage normalization, Hydranautics normalizes differential pressure, water transport coefficient and salt transport coefficient. Normalized permeate flow has the same common equation that depends upon NDP and TCF. TCF is calculated as shown in Eq. (S49):

$$\text{TCF}=K\times\left(\frac{1}{298.15}-\frac{1}{T+273.15}\right) \tag{S49}$$

where T is daily measured temperature in °C, K is a factor that depends on membrane model and takes a value of 2,700 for composite membranes. NDP is calculated using the common equation (pressures in psi, 1 bar = 14.5038 psi), as a function of feed-brine and permeate osmotic pressures, which are estimated as shown in Eqs. (S50) and (S51):

$$\pi_{\text{FC}}\left(\text{psi}\right)=\frac{0.03851\times C_{\text{FC}}\times\left(T+273.15\right)}{\left(1000-\left(\frac{C_{\text{FC}}}{1000}\right)\right)} \tag{S50}$$

$$\pi_{P}\left(\text{psi}\right)=\frac{0.03851\times C_{P}\times\left(T+273.15\right)}{\left(1000-\left(\frac{C_{P}}{1000}\right)\right)} \tag{S51}$$

where feed-brine average concentration C_{FC} is $C_{\text{FC}}=C_{F}\times\text{CF}_{\text{lm}}$ and CF_{lm} is calculated as shown in Eq. (S52):

$$\text{CF}_{\text{lm}}=\frac{\ln\left(\frac{1}{1-Y}\right)}{Y} \tag{S52}$$

where Y is recovery (Q_P/Q_P+Q_C). Feed concertation (C_F) and permeate concentration (C_P) are calculated as a function electrical conductivity (μS/cm). Normalized salt passage is normalized using Eq. (S53):

$$\text{SP}_{n}=\text{SP}_{t}\times\frac{Q_{P,t}\times\text{TCF}_{0}}{Q_{P,0}\times\text{TCF}_{t}} \tag{S53}$$

where t and 0 refer to time = t and time = 0, respectively. SP_t is stable (actual) salt passage at any time = t, calculated as $\text{SP}_t=C_P/C_{\text{FC}}$ and stable salt rejection can be calculated as SR_t = 1–SP_t normalized differential pressure is calculated in Hydranautics approach as shown in Eq. (S54):

$$\text{DP}_{n}\left(\text{bar}\right)=\left(\frac{\text{DP}_{t}\times\left(\frac{Q_{P,0}}{2}+Q_{C,0}\right)^{1.4}}{\left(\frac{Q_{P,t}}{2}+Q_{C,t}\right)^{1.4}}\right)\times\left(1+0.01\times\left(T-25\right)\right) \tag{S54}$$

where DP_t is differential pressure at time = t in bar, Q_P and Q_C are permeate and concentrate flowrates, respectively. Normalized water transport coefficient (A) is calculated in m/s·kPa as shown in Eq. (S55):

$$A_{n}\left(\text{m/s}.kPa\right)=\frac{0.00000006849}{\text{TCF}_{t}\times\text{NDP}_{t}\left(\text{psi}\right)\times\text{Flux}_{t}\left(\text{gfd}\right)} \tag{S55}$$

where NDP is converted to psi units (1 bar = 14.5038 psi). System flux in GFD is calculated as shown in Eq. (S56):

$$\text{Flux}\left(\text{gfd}\right)=\frac{1440\times Q_{P,t}\left(\text{gpm}\right)}{\text{Total Membrance Area}\left(ft^{2}\right)} \tag{S56}$$

Normalized salt transport coefficient (B) is also normalized as shown in Eq. (S57):

$$B_{n}\left(\text{m/s}\right)=\frac{Q_{P,t}\left(\text{gpm}\right)\times C_{P,t}\left(\text{mg/L}\right)}{\text{TCF}_{t}\times264.17\times60\times\begin{pmatrix}\text{No. of Elements per PV}\\ \times\text{No. PVs per Stage}\\ \times\text{Element Area}\left(ft^{2}\right)\\ \times0.0929\end{pmatrix}\times\left(C_{\text{FC},t}-C_{P,t}\right)} \tag{S57}$$

where $Q_{P,t}$ is converted to gpm (1 m^3/h = 4.40286 gpm). Number of elements per pressure vessel and number of pressure vessels per stage are general setup inputs for normalization.

S8. Details of Vontron normalization method

Vontron normalization approach consists of normalized permeate flow and normalized salt rejection. In normalized permeate low, NDP is calculated using pressures in psi. Osmotic pressures of feed-brine and permeate are calculated as shown in Eqs. (S58) and (S59):

$$\pi_{FC}\left(\text{psi}\right)=\frac{0.03851\times C_{FC}\times\left(T+273.15\right)}{\left(1000-\left(\frac{C_{FC}}{1000}\right)\right)} \tag{S58}$$

$$\pi_{P}\left(\text{psi}\right)=\frac{0.03851\times C_{P}\times\left(T+273.15\right)}{\left(1000-\left(\frac{C_{P}}{1000}\right)\right)} \tag{S59}$$

where T is measured temperature in °C, and C_{FC} is feed-brine average concentration calculated as shown in Eq. (S60):

$$C_{FC}\left(\text{mg/L}\right)=C_{F}\times\frac{\ln\left(\frac{1}{1-Y}\right)}{Y} \tag{S60}$$

where Y is recovery (Q_P/Q_F). Feed TDS C_F (mg/L) and permeate TDS C_P (mg/L) are calculated as shown in Eq. (S61):

$$C\left(\text{mg/L}\right)=\left(0.0000000009\times\text{EC}\times\text{EC}\right)+\left(0.47\times\text{EC}\right)+0.0072 \tag{S61}$$

where C is feed or permeate concentration in mg/L, and EC is feed or permeate electrical conductivity in μS/cm. Normalized salt rejection is calculated as shown in Eq. (S62):

$$\text{SR}_{n}=1-\left(C_{P,t}\times\frac{Q_{P,t}}{Q_{P,0}}\times\frac{\text{TCF}_{0}}{\text{TCF}_{t}}\times\frac{C_{\text{FC},0}}{C_{\text{FC},t}}\times\frac{1}{C_{F,0}}\right) \tag{S62}$$

where $C_{P,t}$ is permeate TDS at time = t, $C_{F,0}$ is feed TDS at time = 0. This formula is similar to DOW one. Further actual salt passage is defined as SPa = $C_{P,t}/C_{\text{FC},t}$.

S9. Gap analysis

Parameter	Sensors ID
Inlet conductivity	*zz*ACT13W13D*xxx*
Inlet temperature	*zz*TIT13W13D*xxx* or *zz*TIT13W04D001
Inlet flowrate	*zz*FIT13W05D*xxx* + 01FIT13W14D*xxx*
Inlet pressure	*zz*PIT13W08D*xxx*
Brine flowrate	*zz*FIT13W05D*xxx* + *zz*FIT13W14D*xxx* – {*zz*FIT14W05D*xxx* + (Σ01FIT18W03D*xxx*)/N + (Σ*zz*FIT14W16D*xxx*)/N + 0.1*x* (Σ*zz*FIT14W16D*xxx*)/N}
Brine pressure	*zz*PIT18W01D*xxx*
Permeate conductivity	(*zz*ACT14W03D*xxx* + *zz*ACT14W04D*xxx*)/2
Permeate flowrate	*zz*FIT14W05D*xxx* + (Σ*zz*FIT18W03D*xxx*)/N + (Σ*zz*FIT14W16D*xxx*)/N + 0.1x (Σ*zz*FIT14W16D*xxx*)/N
Permeate pressure	*zz*PIT14W03D*xxx*

S10. Membrane autopsy comparison with RO-TRACK

Project-train	RO-TRACK	Membrane autopsy
Plant AD2 – Train 4	Analytics results CIP prediction The NDP's trend is increasing from 2021-04-30 20:00:00 to 2021-06-05 20:00:00. The CIP or any other action should be done immediately. Trend From 2021-04-30 20:00:00 to 2021-06-05 20:00:00: The NDP's trend is increasing. The NPF's trend is decreasing. The NSP's trend is decreasing. The possible cause is organic fouling (NOM), inorganic (metal, colloidal) and/or membrane compaction.	Results of the autopsy reveal that the membrane surface was organically fouled (~55%), as biofouling.
Plant RAB3 – Train 3	Analytics results CIP prediction The NPF's trend is decreasing from 2022-02-14 20:00:00 to 2022-03-22 20:00:00. The CIP or any other action should be done immediately. Trend From 2022-02-14 20:00:00 to 2022-03-22 20:00:00: The NDP's trend is increasing. The NPF's trend is decreasing. The NSP's trend is increasing. The possible cause is chlorine damage, inorganic fouling (metal, mineral, colloidal), biological fouling, and/or hydrocarbon fouling.	It is assumed that organic composition of foulant around 48%. (inorganic composition: around 52%).